Electronic structure of $La_{1-x}Sr_xCrO_3$

K. Maiti and D. D. Sarma
Solid State and Structural Chemistry Unit, Indian Institute of Science, Bangalore 560 012, India
(Received 29 March 1996)

$LaCrO_3$ is a wide-band-gap insulator which does not evolve to a metallic state even after hole doping. We report electronic structure of this compound and its Sr substituents investigated by photoemission and inverse photoemission spectroscopies in conjunction with various calculations. The results show that $LaCrO_3$ is close to the Mott-Hubbard insulating regime with a gap of about 2.8 eV. Analysis of Cr 2*p* core-level spectrum suggests that the intra-atomic Coulomb interaction strength and the charge-transfer energy to be 5.0 and 5.5 eV, respectively. We also estimate the intra-atomic exchange interaction strength and a crystal-field splitting of about 0.7 and 2.0 eV, respectively. Sr substitution leading to hole doping in this system decreases the charge-excitation gap, but never collapses it to give a metallic behavior. The changes in the occupied as well as unoccupied spectral features are discussed in terms of the formation of local Cr^{4+} configurations arising from strong electron-phonon interactions. [S0163-1829(96)01835-8]

I. INTRODUCTION

The phenomenon of metal-insulator transition, particularly in transition-metal–oxide systems has been investigated for many decades.[1] Specifically compounds based on the 3*d* transition-metal perovskite oxides with the general formula ABO_3 have drawn considerable interest in view of their interesting transport and magnetic properties.[2–6] Stoichiometric perovskite oxides $LaMO_3$ with M=Ti–Co are insulating. Most of these insulating oxides can be driven into a metallic state by changing the oxygen stoichiometry or by substituting a divalent cation such as Sr^{2+}, Ca^{2+}, or Ba^{2+} in place of La^{3+} thereby effectively doping carriers into the system. Thus, it is interesting to note the anomalous behavior of two doped systems, $La_{1-x}Sr_xCrO_3$ and $La_{1-x}Sr_xFeO_3$ which do not undergo the insulator-to-metal transition even at the maximum possible extent of hole doping. In this context, it is important to note that while all the $LaMO_3$ compounds (M=Ti–Fe) have basically an antiferromagnetic arrangement of the spins at the transition-metal sites, the hole-doped metallic compounds $La_{1-x}Sr_xMO_3$, exhibit either a ferromagnetic ($LaMnO_3$) or a Pauli paramagnetic ($LaTiO_3$ and $LaVO_3$) ground state. Significantly, the two solid solutions, $La_{1-x}Sr_xCrO_3$ and $La_{1-x}Sr_xFeO_3$, which remain insulating in the presence of hole doping, continue to have an antiferromagnetic ground state for all values of x. Thus, it is natural to assume a close connection between the antiferromagnetism and the insulating behavior in all these systems. Recently, it has been reported[7] that $La_{1-x}Sr_xFeO_3$ exhibits a metallic resistivity with temperature above the Néel temperature. In contrast, $La_{1-x}Sr_xCrO_3$ continues to show an insulating behavior even very far above the Néel temperature.[8] The electric and magnetic properties as well as the detailed electronic structure of $La_{1-x}Sr_xFeO_3$ series have been studied extensively for the past few years.[9] Surprisingly, the electronic structure of the more anomalous series $La_{1-x}Sr_xCrO_3$ has not been investigated in any detail. Thus, we have undertaken a detailed electron spectroscopic investigation of this series in order to obtain microscopic information concerning the electronic structure.

Pure $LaCrO_3$ is a slightly distorted pseudocubic perovskite oxide, which exhibits a phase transition from orthorhombic to rhombohedral structure around 560 K. While the activation energy measured from transport properties[10] is about 0.18 eV, this green-colored insulator shows a gap of about 3.3 eV (Ref. 11) from optical measurements. The color of the compound turns black even with a very small amount of Sr doping (about $\sim$ 0.1%), suggesting a strong reduction in the optical gap on hole doping. The activation energies obtained from the resistivity measurements remain almost the same ($\sim$0.1–0.2 eV) for different extents of hole doping.[8,10] The temperature dependence of resistivity suggests that the electrical conduction in this system is primarily due to the hopping of small polarons, arising from a strong electron-phonon interaction. The doped charge carriers are believed to distort the lattice locally, becoming self-trapped in the resulting potential well. Magnetic susceptibility measurements show that $LaCrO_3$ is antiferromagnetic with a Néel temperature of 275 K.[12] The magnetic moment at the transition-metal site is about $3.85\mu_B$ which is very close to the value ($3.87\mu_B$) expected from the d^3 high spin configuration of Cr^{3+} in the octahedral environment. Sr substitution decreases the effective magnetic-moment considerably; these are about $2.41\mu_B$, $2.11\mu_B$, $1.93\mu_B$, and $2.36\mu_B$ at room temperature for x = 0.1, 0.2, 0.3, and 0.5, respectively, in $La_{1-x}Sr_xCrO_3$.[8,13] High-temperature resistivity measurements show that the hole-doped compounds exhibit negative temperature coefficient of resistivity even up to 1900 K, indicative of a semiconducting behavior at all temperatures. In order to obtain a microscopic description of the electronic structure in these systems, we have carried out a detailed investigation using x-ray photoemission (XP), ultraviolet photoemission (UP), and bremsstrahlung isochromat (BI) spectroscopic measurements, in conjunction with *ab initio* band-structure calculations, as well as parametrized many-body calculations.

II. EXPERIMENT

The samples of $La_{1-x}Sr_xCrO_3$ ($x=0.0$, 0.1, 0.2, 0.3, and 0.5) were prepared by the solid-state reaction using predried La_2O_3, Cr_2O_3, and $SrCO_3$ in appropriate proportions. The reactants were ground together and heated at 950 °C for about 24 h in air. This was followed by heating at 1000 °C, 1100 °C, and 1350 °C for about 12 h each with grindings in between. Finally, the samples were pelletized and heated at 1350 °C for about 72 h with several grindings in between. In order to get well-sintered homogeneous samples, the final sintering of all the pellets were carried out at 1600 °C for 24 h followed by slow cooling. The x-ray diffraction pattern showed a single orthorhombic phase for x up to 0.3. For $x=0.5$ there is a rhombohedral distortion. The lattice parameters match well with the reported data.[14] These compounds were further characterized by resistivity and susceptibility measurements over a wide range of temperatures; the results obtained were found to be in good agreement with the reported values.[13]

XP, UP, and BI spectroscopic measurements were carried out in a commercial electron spectrometer from VSW Scientific Instruments Ltd. All the experiments were carried out at room temperature. The sample surface was repeatedly scraped *in situ* with an alumina file to clean the surface; the cleanliness was monitored by the impurity feature at the higher-binding-energy side of the O 1*s* spectrum as well as by the C 1*s* signal. Such features indicating various contaminations were below the level of detection in every case. The XP spectra are recorded using Mg $K\alpha$ (1253.6 eV) radiation with a resolution of 1.0 eV. The Cr 2*p* core-level spectra have been collected using Al $K\alpha$ radiation in order to avoid the La $M_{45}N_{45}N_{45}$ Auger feature and some very weak Auger features due to Cr. The UP spectra are obtained using a He discharge lamp and the resolution in this technique was better than 100 meV. BI spectra have been recorded monochromatizing the emitted photons at 1486.6 eV with a total resolution of 0.8 eV.

Due to uneven charging of the wide-band-gap insulator, $LaCrO_3$, the recorded spectra exhibited multiple ghost peaks in the x-ray photoemission technique; this problem could be substantially eliminated by using a low-energy electron flood-gun. However, the spectra thus recorded appeared to be somewhat broader than expected. Moreover, it was not possible to record the UP and BI spectra of $LaCrO_3$ due to intense charging effects. The doping of hole states by substitution of La^{3+} by Sr^{2+} decreases the charge-excitation gap as well as the resistivity of the samples. In these substituted compounds, it was not necessary to use the flood-gun in order to neutralize the charges created by the photoemission process. Our analysis shows that the main difference between the spectrum of $La_{0.9}Sr_{0.1}CrO_3$ and that of $LaCrO_3$ is a broadening, arising from the charging effects in the latter, while the spectral signatures are very similar. Thus, we take the spectrum of $La_{0.9}Sr_{0.1}CrO_3$ as the reference spectrum for comparison with other higher-doped compounds in order to understand the effect of doping in this system.

Spin-polarized scalar-relativistic linearized muffin-tin orbital calculation within the atomic sphere approximation (LMTO-ASA) for $LaCrO_3$ was performed in the orthorhombic phase with 20 atoms per unit cell, the lattice constants being $a=5.512$ Å, $b=5.476$ Å, and $c=7.752$ Å.[14] The sphere radii used are 1.8840, 1.3529, and 1.1748 Å for La, Cr, and O sites, respectively; no empty sphere was required in the calculation, in order to satisfy the volume-filling criterion. In this semirelativistic calculation, convergence was obtained self-consistently using *s*, *p*, *d*, and *f* basis at each atomic sphere with 80 *k* points in the irreducible part of the Brillouin zone. The energies E_ν^l for each angular momentum partial wave were chosen to be the center of gravity of the occupied part of the corresponding partial density of states (DOS). The calculation was carried out for the observed *G*-type antiferromagnetic state and an insulating state was obtained for this structure with a finite gap between the highest occupied and the lowest unoccupied levels.

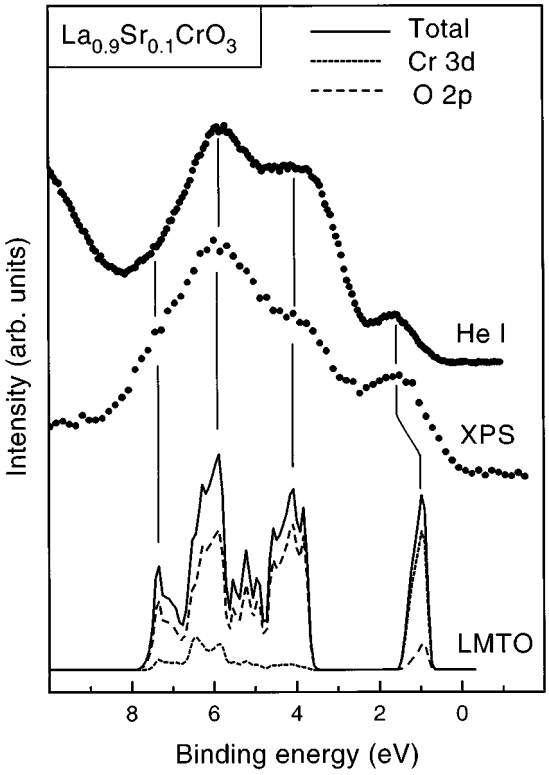

FIG. 1. Valence-band spectra of $La_{0.9}Sr_{0.1}CrO_3$ with incident photon energies 21.2 eV (He I) and 1253.6 eV (XPS) along with the DOS obtained from LMTO-ASA band-structure calculations.

III. RESULTS AND DISCUSSION

We show the XP and UP valence-band spectra of $La_{0.9}Sr_{0.1}CrO_3$ compared to the calculated total DOS along with the Cr *d* and O *p* partial DOS obtained from spin polarized LMTO-ASA band structure calculations for $LaCrO_3$ in Fig. 1. The calculated DOS had to be shifted by about 0.5 eV in order to align the most intense feature to that of the experimental spectra at about 5.8 eV; this is necessitated by the well-known underestimation of band gaps in such band-structure calculations.[15,16] The experimental spectra exhibit three distinct features at 1.7, 4.0, and 5.8 eV, respectively. The intensity of the 1.7-eV feature increases relative to the 5.8-eV feature with an increase in the photon energy from 21.2 eV (He I) to 1253.6 eV (XPS); since the relative cross-

section of transition-metal 3*d* states compared to oxygen 2*p* states increases with an increasing photon energy,[17] it is clear that the 1.7-eV feature in the spectra arise primarily from the Cr *d* photoemission, while the higher-binding-energy features have primarily an oxygen *p* character. It is seen that the relative intensity of the 4-eV binding-energy feature arises from interactions mainly within oxygen 2*p*-states with minimal contribution from Cr *d*-states; such states are often termed as the nonbonding oxygen *p* states. The spectral feature at about 6-eV binding-energy is attributed to dominant oxygen *p*-character arising from the bonding interaction between Cr *d* and O *p* states. These interpretations are clearly supported by the calculated total DOS and partial DOS shown in Fig. 1. Thus, we find that the leading feature in the occupied part of the DOS has primarily Cr *d* character and thus, compares favorably with the experimental observations on the leading spectral feature at 1.7 eV; however, the energy position of this peak appears to be underestimated in the calculation, due to an inadequate treatment of electron correlations in such effective single-particle band-structure approaches. The DOS in the energy range between 3.5 and 5 eV is in good agreement with the experimentally observed shoulder at about 4.0 eV; the partial DOS clearly shows a very small contribution of Cr *d* states in this energy range, suggesting the nonbonding character. The main peak in the experimental spectra at about 6 eV is also in good agreement with the DOS in the energy range between 5.5 and 6.8 eV. While these states have dominant oxygen *p* character, there is a finite Cr *d* admixture in this energy range, suggesting the Cr *d*–O *p* bonding character here. Thus, it appears that the photoemission valence-band spectrum as well as its photon-energy dependence are basically consistent with band-structure results. It is also interesting to note that the band-structure calculation indeed obtains an insulating ground state for this compound, in agreement with the experiments; however, the calculated gap is about 1.0 eV in contrast to a measured optical gap of about 3.3 eV.[11] Thus, it appears that while a band gap would form in this material even due to the magnetic and geometric arrangements of the atoms, strong electron-electron interaction effects further enhance the band-gap considerably. One of the signatures of this enhanced bandgap due to correlation effects is the shift of the primarily Cr *d*-related feature in the DOS at about 1.0 eV to about 1.7 eV in the experimental spectra (see Fig. 1). The character of the leading ionization states derived primarily from Cr *d* levels suggests that $LaCrO_3$ should be classified as a Mott-Hubbard insulator;[18–20] this is consistent with an analysis of the core-level photoemission spectrum in $LaCrO_3$.[21]

In order to probe the unoccupied parts of the electronic structure in this series of compounds, we have recorded the BI spectra of these compounds. We show the BI spectrum of $La_{0.9}Sr_{0.1}CrO_3$, compared to the spin-polarized Cr *d* partial DOS in Fig. 2. The most intense peak in the experimental spectrum, at about 8.1 eV, is due to the La 4*f* signal. The weak features between approximately 0 and 6 eV above E_F arise primarily from Cr 3*d*-states; however, the spectral features in this region, particularly near the higher-energy end, are strongly distorted due to the tailing of the intense 4*f* signal. In spite of this difficulty, the feature marked *A* in Fig. 2 near 4.5 eV due to the upper Hubbard band can be clearly

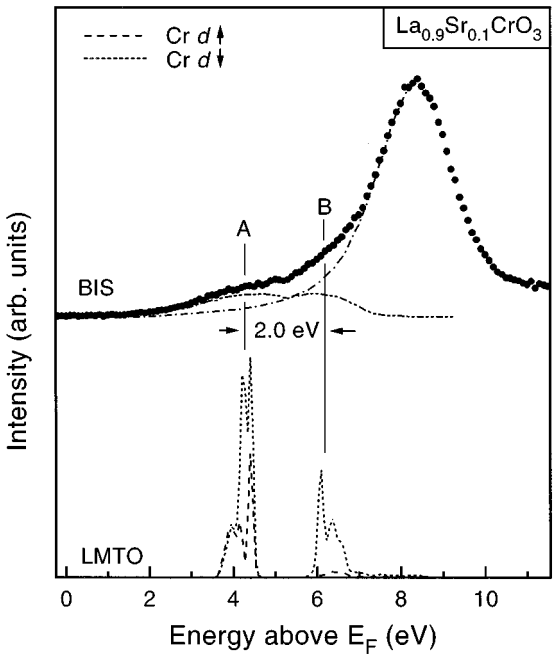

FIG. 2. BI spectrum of $La_{0.9}Sr_{0.1}CrO_3$ and the calculated DOS corresponding to the unoccupied part of Cr *d*-like states to show the characters of different features of the experimental spectrum.

seen in the experimental spectrum. The other spectral feature marked *B* in the figure is barely discernible as a weak shoulder on the low-energy tail of the La 4*f* signal. In order to compare the calculated DOS with the spectroscopic features corresponding to the unoccupied parts, we have found that the band-structure results systematically overestimate the features by about 25% for a wide range of transition-metal oxides.[15,16] Specifically, such an overestimation has been established in the case of $LaCrO_3$ by comparing the x-ray-absorption spectrum with calculated results.[22] Thus, we contract the energy scale uniformly by 25% for the calculated Cr *d*-partial DOS and compare it with the experimental spectrum in Fig. 2. These spin-polarized partial DOS suggest both up- and down-spin states contribute to the experimental feature *A*. Thus, we contribute this spectral feature to transitions into the Cr $t_{2g\downarrow}$ and $e_{g\uparrow}$ states of the Cr^{3+} $t^3_{2g\uparrow}t^0_{2g\downarrow}e^0_{g\uparrow}e^0_{g\downarrow}$ configuration. The spectral feature *B* arises only from transitions to the down-spin states, as suggested by the partial DOS in the figure, and thus corresponds to the Cr $e_{g\downarrow}$ states. Thus, the energy separation of about 2.0 eV between the features marked *A* and *B* in Fig. 2, being the energy difference between $t_{2g\downarrow}$ and $e_{g\downarrow}$ states, is a measure of the crystal-field splitting in $LaCrO_3$. We can also estimate the strength of the exchange splitting in this system from the fact that the partial DOS corresponding to $t^1_{2g\downarrow}$ and $e^1_{g\uparrow}$ states, in the presence of a $t^3_{2g\uparrow}$ ground-state configuration, appear to be very close in energy, giving rise to a single high-intensity feature (*A* in Fig. 2). The energy difference for a transition into the $t_{2g\downarrow}$ and $e_{g\uparrow}$ states is given by $(3J-q)$, with J being the exchange interaction strength and q the crystal-field-splitting. The results in Fig. 2 suggest that this energy difference is small and thus, $J \approx q/3$ being in the order of 0.7 eV.

We can combine the results of Figs. 1 and 2 corresponding to the spectral features of the occupied and the unoccu-

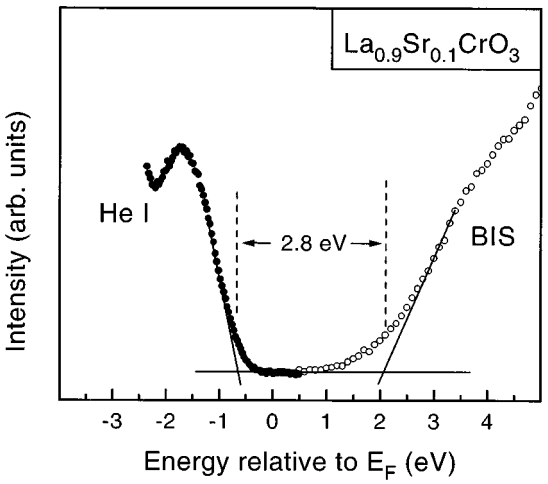

FIG. 3. The He I valence-band and BI spectra of $La_{0.9}Sr_{0.1}CrO_3$ near Fermi energy to get an estimate of the band-gap approximately 2.8 eV.

pied parts of the electronic structure, to obtain an estimate of the charge-excitation gap in these materials. We have combined the UP and BI spectra of $La_{0.9}Sr_{0.1}CrO_3$ with a common Fermi energy in Fig. 3. It is impossible to determine the band edges precisely from these experimental spectra, since the bands and the band edges are broadened in the recorded spectra due to the presence of finite resolution in the experimental technique. Thus, we adopt an approach which has been useful in the past in determining the band edges in $LaMnO_3$ (Ref. 23) and $LaFeO_3$ (Ref. 9) and is illustrated in Fig. 3. This procedure yields an estimate of the band-gap to be about 2.8 eV. This value is consistent with the green color of the stoichiometric sample. The optical gap of $LaCrO_3$ has been estimated to be about 3.3 eV.[11] Considering the uncertainties in defining the band edges in the present experiments, as well as in the optical absorption experiment, these two estimates of the intrinsic gap in this material appear to be within the experimental error. Thus, the gap estimated from dc-conductivity measurements as 0.2 eV (Refs. 8 and 10) is most probably due to the presence of nonstoichiometry even in the parent compound with nominal composition of $LaCrO_3$; this would not be surprising in view of the fact that most of the $LaMO_3$ compounds are known to have extensive cationic and/or anionic vacancies.

We show the core-level photoemission spectrum in the Cr $2p$ region of $LaCrO_3$ in Fig. 4. The intense peaks at about 345 and 355 eV binding energies are due to Cr $2p_{3/2}$ and $2p_{1/2}$ main signals, respectively. In addition to these, one can clearly see the weak intensity peak at about 367 eV which is the satellite accompanying the $2p_{1/2}$ main peak at 355 eV. Thus, the satellite energy separation from the main peak is approximately 12 eV. The spin-orbit splitting of the Cr $2p$ main peak is around 10 eV; this implies that the satellite accompanying the Cr $2p_{3/2}$ main peak strongly overlaps with the Cr $2p_{1/2}$ main peak; an inspection in the Cr $2p_{1/2}$ signal in Fig. 4 indeed reveals a strong asymmetric broadening of this feature near about 357-eV binding energy. This clearly suggests that the satellite accompanying the Cr $2p_{3/2}$ feature is responsible for this asymmetric broadening; we have indicated the approximate position of this satellite feature with a

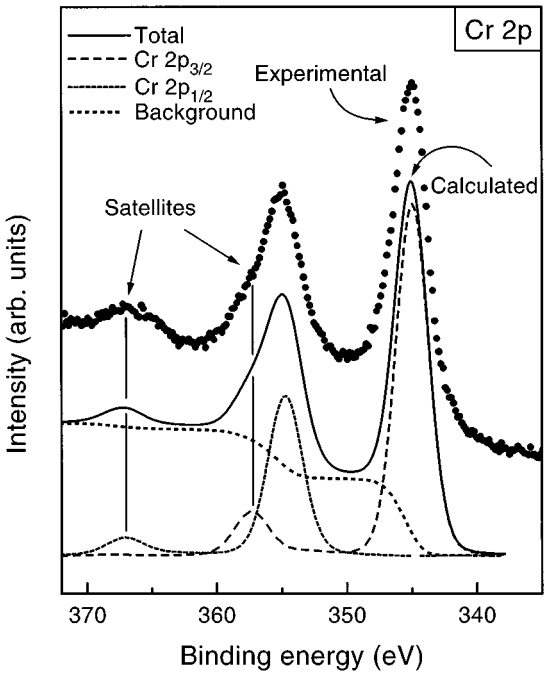

FIG. 4. The core-level spectrum of $LaCrO_3$ and the calculated spectrum using cluster approximation.

vertical line in the figure. In order to provide a quantitative description of the core-level spectrum, we have simulated the spectrum within the cluster-model for various values of the parameter strengths in the model Hamiltonian along well-known methods in the literature.[24,25] We have included configurations d^3, $d^4\underline{L}^1$, $d^5\underline{L}^2$, $d^6\underline{L}^3$, and $d^7\underline{L}^4$ in the configuration interaction calculations; here $\underline{L}^1$ denotes a hole in the ligand level. It is well known that wide ranges of parameter values would be compatible with any given experimental spectrum arising from the nonuniqueness of the solution.[26] In order to obtain somewhat better defined estimates of the various interaction strengths, we fixed the hybridization strength between Cr $3d$ and O $2p$ to the estimate obtained from *ab initio* band-structure calculations.[27] Thus, the usual Slater-Koster parameter, $(pd\sigma)$ has been taken to be 2.37 eV. We find a good description of the experimental spectrum for the charge transfer energy $\Delta=5.5$ eV and intra-atomic Coulomb interaction strength $U_{dd}=5.0$ eV. The spectrum calculated for these values of the parameter strengths is shown in Fig. 4, along with the spin-orbit components and the satellite features. It is obvious from the figure that the calculated spectrum describes the experimental one well, including the higher-energy asymmetry of the $2p_{1/2}$ signal. We have also calculated the ground-state character of this compound on the basis of these parameter strengths. Thus, we obtain 46%, 42%, 11%, and 1% of d^3, $d^4\underline{L}^1$, $d^5\underline{L}^2$, and $d^6\underline{L}^3$ configurations, respectively, in the ground-state of $LaCrO_3$. This suggests an average d-occupancy n_d of about 3.7; since it has been found[26] that n_d is given rather reliably by such calculations, this value of n_d indicates that $LaCrO_3$ has strongly mixed valent character. Our calculations further show that the final state corresponding to the main peak in the Cr $2p$ spectral region has about 20%, 25%, 33%, 10%, and 12%, while the satellite region has 63%, 3%, 5%, 10%, and 19%

of d^3, $d^4\underline{L}^1$, $d^5\underline{L}^2$, $d^6\underline{L}^3$, and $d^7\underline{L}^4$ configurations, respectively. This suggests that the nature of the satellite in this compound is that of an unscreened state with a large d^3 character, while the main peak represents a charge-transfered well-screened state with less d^3 character compared to the ground-state.

We now turn to the question of hole doping in this system by chemical substitution of La^{3+} by Sr^{2+} and its consequence on the electronic structure. In Fig. 5 we show the valence-band UP spectra of $La_{1-x}Sr_xCrO_3$ for $x = 0.1$, 0.2, 0.3, and 0.5. The various spectra in Fig. 5(a) have been normalized to the integrated area up to about 8 eV binding-energy. We find that the intensities of the features near 2 and 6 eV binding-energies decrease compared to the nonbonding oxygen p-band-feature at about 4 eV with increasing Sr substitution. Sr doping introduces holes in the Mott-Hubbard insulator $LaCrO_3$ and the holes are expected to have primarily Cr d character. Thus, the decrease in the spectral intensities related to Cr d-admixed states in the occupied part compared to the intensity of the spectral feature of the oxygen nonbonding p band is consistent with depletion of Cr d occupancy with progressive hole doping. In order to monitor changes in the leading edge of the occupied states on doping, we show the spectra over a narrow energy range with improved signal-to-noise ratio in Fig. 5(b). In this case, we have normalized all the spectra at the maximum intensity near 2 eV. None of the spectra with x varying between 0.1 and 0.5 exhibits any intensity at the Fermi energy, and there is clear evidence of a finite gap in each of these cases. This is consistent with the results of conductivity measurements, which clearly show an insulating activated charge transport at every composition in spite of hole doping in $LaCrO_3$. However, we find a systematic shift of the peak position and the leading edge of the photoemission signal towards E_F with increasing Sr substitution; this is illustrated by vertical lines marking the peak positions and in the inset by overlapping the spectra of two extreme compositions. The peak position is found to shift by about 80 meV between the extreme compositions; the shift in the leading edge is also about the same. Since the various spectra are referred to a common Fermi energy in Fig. 5(b), these shifts in the spectral feature clearly indicate a movement in the Fermi energy by about 80 meV towards the occupied states with increasing hole doping. This estimate is in very good agreement with the observed decrease in the activation energy by about 80 meV when Sr content is changed from 0.1 to 0.5.[8,10] We shall discuss the microscopic origin of this phenomenon later in the text together with the changes in the unoccupied part of the spectra.

We show the overview BI spectra of this series in Fig. 6. In every case, the La 4f signal is found at about 8.1 eV. Weaker intensity signals at lower energies corresponding to the upper Hubbard band exhibit some systematic changes across the series; for example, there are new states arising due to hole doping at about 2.6 eV on the lower-energy side of the upper Hubbard band of $LaCrO_3$ as illustrated in the inset I in Fig. 6 by comparing the two extreme compositions. In order to compare the spectral changes close to the E_F, we have collected BI spectra over a narrow energy range with considerably improved signal-to-noise ratio. We show this narrow energy range on an expanded scale in the inset II of Fig. 6, where we also show the base line for each of the spectra. From this figure it is clear that the doped holes introduce states close to the E_F, along with states near 2.6 eV (see inset I). Both these features are found to grow in inten-

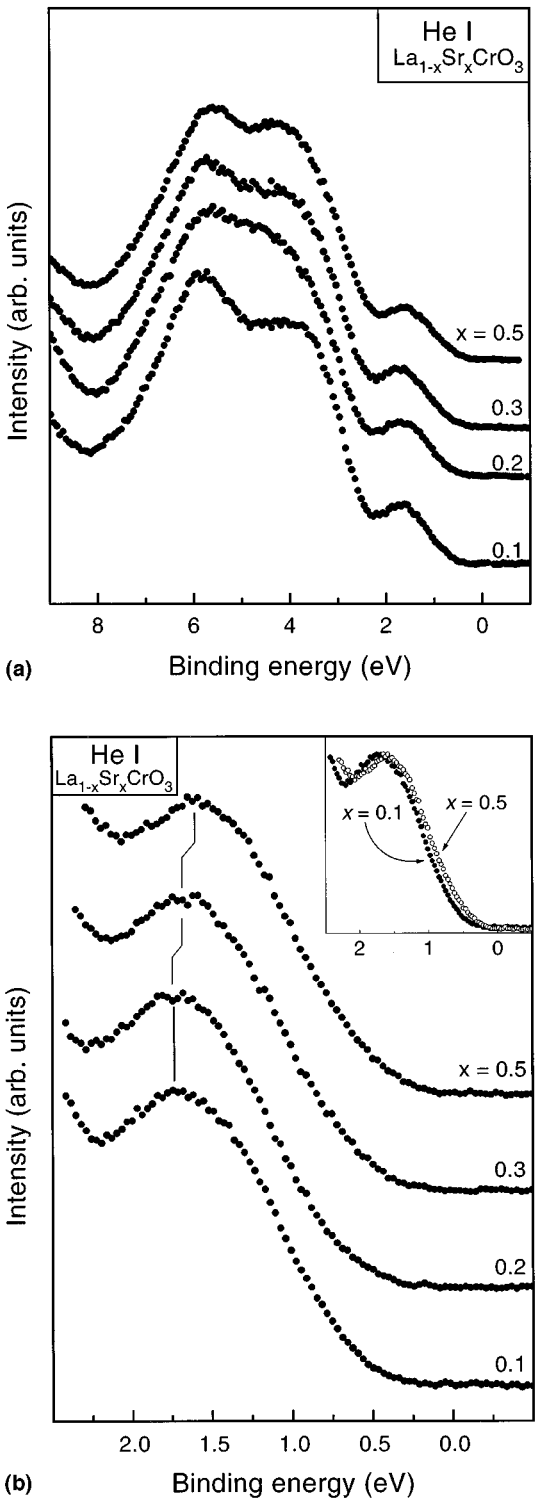

FIG. 5. (a) The He I spectra of $La_{1-x}Sr_xCrO_3$ ($x=0.1$, 0.2, 0.3, 0.5). (b) The He I spectra of $La_{1-x}Sr_xCrO_3$ ($x=0.1$, 0.2, 0.3, 0.5) at the near-Fermi-energy region. In the inset we show the shift of the Cr d-like feature towards the Fermi energy with x.

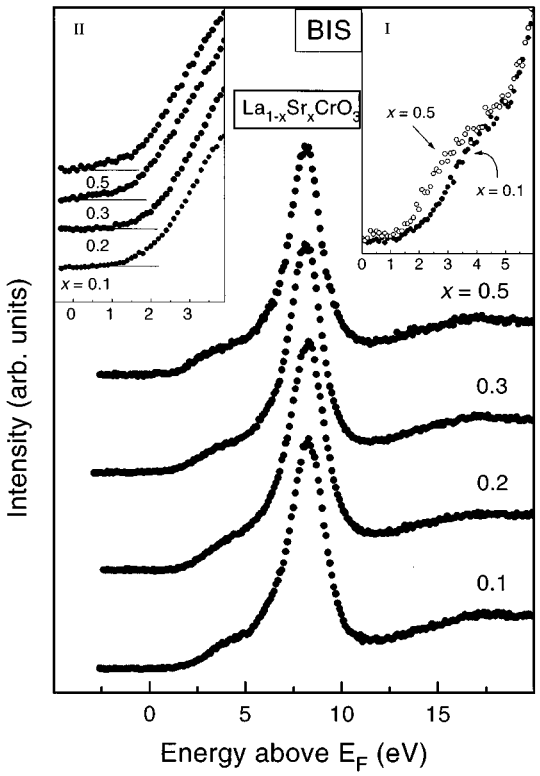

FIG. 6. The BI-spectra of $La_{1-x}Sr_xCrO_3$ (x=0.1,0.2,0.3, 0.5). In inset I we show the near-E_F region of $La_{0.9}Sr_{0.1}CrO_3$ and $La_{0.5}Sr_{0.5}CrO_3$ to show the feature around 2.6 eV. In inset II we show the near-E_F region with a very large signal-to-noise ratio to show the growing feature around 1.0 eV above E_F.

sity systematically with increasing x establishing these as doped hole states. However, even at the highest concentration of Sr (x=0.5), the E_F lies in a region of no spectral intensity, a behavior that is typical of insulators and is consistent with the transport properties of this series. It is to be noted here that the insulating nature of the doped compounds in this series is not likely to be primarily due to the formation of a Mott-Hubbard gap due to strong electron correlation alone, since the insulating state persists at arbitrary hole doping or for all values of x in $La_{1-x}Sr_xCrO_3$. Thus, the insulating nature of these compounds may either arise from an Anderson localization or from a localization of the doped holes due to the presence of impurity potentials. For each composition, we find clear evidence of a gap with no density of states at and near E_F in Figs. 5 and 6. Thus, it does not appear to be a case of Anderson localization either; in this case one would expect a finite DOS at E_F, though the states are localized. In view of these considerations, it appears clearly that the insulating nature of the doped samples arises from a localization of the doped holes by the impurity potential. This process is possibly aided by the presence of strong electron-phonon interaction leading the formation of small polarons as suggested in earlier studies.[8,10,22] Figure 6 shows that the induced doped hole states in $La_{1-x}Sr_xCrO_3$ are localized in two groups, centered at about 1 and 2.6 eV above E_F. These states, with no perceivable weight at E_F, do not introduce a metal-insulator transition as in any other $La_{1-x}Sr_xMO_3$ (M is a 3d-transition element) series.[23,28] However, the hole doped states appearing at about 1 eV and extending significantly towards E_F are clearly situated in the bandgap of the parent insulating compound (see Fig. 4) and thus, give rise to a strong reduction in the intrinsic bandgap. These states are directly responsible for the observation that substitution of Sr in place of La leads to a change in color from green to black in $La_{1-x}Sr_xCrO_3$. Since the doped holes are localized in a Mott-Hubbard insulator, these emerging spectral features with hole doping are attributed to the formation of localized Cr^{4+} configuration with a local $t_{2g\uparrow}^2$ configuration. The small spectral intensity progressively growing at about 1 eV with increasing x in $La_{1-x}Sr_xCrO_3$ (see inset II in Fig. 6), is interpreted as transitions into the $t_{2g\uparrow}$ states of Cr^{4+} sites, while the hole doped spectral feature near about 2.6 eV (inset I in Fig. 6) is due to transitions into $t_{2g\downarrow}$ and $e_{g\uparrow}$ states of Cr^{4+} sites. The transitions into the $e_{g\downarrow}$ state of the hole doped site should appear in the vicinity of 5 eV, assuming a crystal-field-splitting of about 2.5 eV for the Cr^{4+} site; however, this small intensity signal is difficult to identify due to the large intensity of the overlapping states in the same energy range. The above interpretation also explains the small but systematic shift of the Fermi energy with increasing x observed in this series [Fig. 5(b)]. It is reasonable to expect that the increasing concentration of Cr^{4+} with x will lead to a broadening of the localized bands. E_F being pinned at the bottom of the Cr^{4+} $t_{2g\uparrow}$ band, an increase in the bandwidth will push E_F to lower energy towards the occupied bands. This will reflect itself as a shift of the leading edge of the valence band towards E_F as shown in Fig. 5(b) and also as a decrease in the activation energy in conductivity measurements as observed in Refs. 8 and 10.

IV. CONCLUSION

In conclusion, we have presented high-energy spectroscopic results for $La_{1-x}Sr_xCrO_3$ with x = 0.0, 0.1, 0.2, 0.3, and 0.5. The core-level spectrum of $LaCrO_3$ has been analyzed in terms of the configuration-interaction model and the parameter strengths controlling the electronic structure of this system have been estimated. The valence-band spectra corresponding to both occupied and unoccupied states have been analyzed with the help of *ab initio* band-structure calculations; these spectra suggest that the intrinsic gap in this material is about 2.8 eV. Hole doping by substitution of La with Sr leads to systematic changes in the valence-band spectra. These changes have been discussed and interpreted in terms of formation of local Cr^{4+} states, where localization of the doped holes, possibly aided by strong electron-phonon interactions, causes the insulating state to survive the doping of holes. These results are discussed in terms of the known transport properties of $La_{1-x}Sr_xCrO_3$.

ACKNOWLEDGMENTS

The authors thank Professor C.N.R. Rao for his continued support and Professor A. Fujimori for helpful discussions. Financial support from the Department of Science and Technology, Government of India is also acknowledged here. One of us (K.M.) is thankful for support from the Council of Scientific and Industrial Research, Government of India.

[1] N. F. Mott, *Metal Insulator Transition*, 2nd ed. (Taylor and Francis, London, 1990).
[2] Y. Tokura, Y. Taguchi, Y. Fujishima, T. Arima, K. Kumagai, and Y. Iye, Phys. Rev. Lett. **70**, 2126 (1993); Y. Fujishima, Y. Tokura, T. Arima, and S. Uchida, Phys. Rev. B **46**, 11 167 (1992).
[3] A. Chainani, M. Mathew, D. D. Sarma, I. Das, and E. V. Sampathkumaran, Physica B **186-188**, 995 (1993).
[4] I. H. Inoue *et al.*, Jpn. J. Appl. Phys. **32**, 451 (1994); A. Fukushima *et al.*, J. Phys. Soc. Jpn. **63**, 409 (1994); M. Onoda *et al.*, Solid State Commun. **79**, 281 (1991).
[5] G. H. Jonker and J. H. Van Santen, Physica **XVI**, 337 (1950); J. H. Van Santen and G. H. Jonker, *ibid.* **XVI**, 599 (1950); R. Mahendiran, A. K. Raychoudhury, A. Cahinani, and D. D. Sarma, Appl. Phys. Lett. **66**, 233 (1995).
[6] R. R. Heikes, R. C. Miller, and R. Mazelsky, Physica **30**, 1600 (1964); C. S. Naiman *et al.*, J. Appl. Phys. **36**, 1044 (1965).
[7] Presented by Y. Tokura *et al.* (unpublished).
[8] D. P. Karim and A. T. Aldred, Phys. Rev. B **20**, 2255 (1979).
[9] A. Chainani, M. Mathew, and D. D. Sarma, Phys. Rev. B **48**, 14 818 (1993); A. Chainani, Ph.D. thesis, I. I. Sc., Bangalore, India, 1993.
[10] J. B. Webb, M. Sayer, and A. Mansingh, Can. J. Phys. **55**, 1725 (1977).
[11] T. Arima, Y. Tokura, and J. B. Torrance, Phys. Rev. B **48**, 17 006 (1993).
[12] K. P. Bansal, S. Kumari, B. K. Das, and G. C. Jain, J. Mater. Sci. **18**, 2095 (1983).
[13] P. Sujatha Devi and M. Subba Rao, J. Solid State Chem. **98**, 237 (1992).
[14] C. P. Khattak and D. E. Cox, Mater. Res. Bull. **12**, 463 (1977).
[15] D. D. Sarma, N. Shanthi, S. R. Barman, N. Hamada, H. Sawada, and K. Terakura, Phys. Rev. Lett. **75**, 1126 (1995).
[16] D. D. Sarma, N. Shanthi, and Priya Mahadevan, Phys. Rev. B **54**, 1622 (1996).
[17] J. J. Yeh, and I. Lindau, At. Data Nucl. Data Tables **32**, 1 (1985).
[18] J. Zaanen, G. A. Sawatzky, and J. W. Allen, Phys. Rev. Lett. **55**, 418 (1985).
[19] D. D. Sarma, H. R. Krishnamurthy, Seva Nimkar, S. Ramasesha, P. P. Mitra, and T. V. Ramakrishnan, Pramana **38**, L531 (1992).
[20] Seva Nimkar, D. D. Sarma, H. R. Krishnamurthy, and S. Ramasesha, Phys. Rev. B **48**, 7355 (1993).
[21] A. E. Bocquet, T. Mizokawa, K. Morikawa, A. Fujimori, S. R. Barman, K. Maiti, D. D. Sarma, Y. Tokura, and M. Onoda, Phys. Rev. B **53**, 1161 (1996).
[22] D. D. Sarma, K. Maiti, E. Vescovo, C. Carbone, W. Eberhardt, O. Rader, and W. Gudat, Phys. Rev. B **53**, 13 369 (1996).
[23] A. Chainani, M. Mathew, and D. D. Sarma, Phys. Rev. B **47**, 15 397 (1993).
[24] D. D. Sarma, Rev. Solid State Sci. **5**, 461 (1991).
[25] D. D. Sarma, Phys. Rev. B **37**, 7948 (1988); D. D. Sarma and A. Taraphder, *ibid.* **39** 11 570 (1989); D. D. Sarma and S. G. Ovchinnikov, *ibid.* **42**, 6817 (1990).
[26] D. D. Sarma, J. Phys. Soc. Jpn. **65**, 1325 (1996).
[27] Priya Mahadevan, N. Shanthi, and D. D. Sarma, Phys. Rev. B (to be published).
[28] A. Chainani, M. Mathew, and D. D. Sarma, Phys. Rev. B **46**, 9976 (1992).